Natural Resources Canada | Ressources naturelles Canada

GEOLOGICAL SURVEY OF CANADA
OPEN FILE 8025

Report on the composition and assemblage of minerals associated with the porphyry Cu-Mo mineralization at the Gibraltar deposit, south central British Columbia, Canada

C.H. Kobylinski, K. Hattori, S. Smith and A. Plouffe

2016

Canada

GEOLOGICAL SURVEY OF CANADA
OPEN FILE 8025

Report on the composition and assemblage of minerals associated with the porphyry Cu-Mo mineralization at the Gibraltar deposit, south central British Columbia, Canada

C.H. Kobylinski[1], K. Hattori[1], S. Smith[2] and A. Plouffe[3]

[1] Department of Earth and Environmental Sciences, University of Ottawa, 25 Templeton St., Ottawa, Ontario
[2] Taseko Gibraltar, 10251 Gibraltar Mine Rd., McLeese Lake, British Columbia
[3] Geological Survey of Canada, 601 Booth Street, Ottawa, Ontario

2016

doi:10.4095/298804

This publication is available for free download through GEOSCAN (http://geoscan.nrcan.gc.ca/).

Recommended citation
Kobylinski, C.H., Hattori, K., Smith, S., and Plouffe, A., 2016. Report on the composition and assemblage of minerals associated with the porphyry Cu-Mo mineralization at the Gibraltar deposit, south central British Columbia, Canada; Geological Survey of Canada, Open File 8025, 30 p. doi:10.4095/298804

Publications in this series have not been edited; they are released as submitted by the author.

Table of Contents

Abstract

Glacial sediments commonly contain resistate heavy minerals, such as zircon, rutile and epidote. To identify the sources of these minerals and use them as a vectoring tool for mineral deposits, it is critical to understand the compositional variations and assemblages of these minerals in mineral deposits and whether they are distinct from those in barren rocks. This paper reports the occurrence and assemblages of igneous and alteration minerals in the Gibraltar porphyry Cu deposit, southcentral British Columbia.

The Gibraltar deposit is the largest of three porphyry-Cu deposits in the region, the others being the Mount Polley mine and the Woodjam prospect. The Gibraltar deposit is hosted by the Granite Mountain batholith and has reserves of over 749 million tons at 0.249% Cu and 0.008% Mo. The batholith is mostly tonalite, with minor variation in modal abundances of felsic and mafic minerals. Igneous minerals are plagioclase, quartz, biotite, hornblende, titanite, zircon and apatite. The mineralization is accompanied by extensive phyllic alteration in the tonalite, which produced illite, quartz, rutile, titanite, magnetite, apatite, chlorite and epidote. Hydrothermal titanite is distinctly different from igneous titanite in crystal habits, optical properties and chemical compositions. Epidote shows a large compositional variation even within one sample from Al-rich (high clinozoisite component) to Fe-rich epidote. Some epidote grains contain significant La and Ce (allanite component), which could be diagnostic of the porphyry mineralization. Preliminary observations suggest the presence of a potassic alteration zone forming hydrothermal biotite, but is now replaced by chlorite.

Introduction

Porphyry Cu mineralization is accompanied by extensive alteration within the host rocks and surrounding country rocks. Some of these minerals are resistant against weathering and erosion. They can be dispersed by glaciers and streams and may occur in glacial and stream sediments. Therefore, the assemblage of minerals common in porphyry Cu deposits in these sediments may vector to a deposit when combined with knowledge of regional ice-flow directions. Among heavy minerals, epidote (a Fe-rich variety of epidote group minerals) has the potential to be useful in mineral exploration. Cooke et al. (2014) reported that spatial variation of epidote chemistry in bedrock can be used to predict the occurrence and size of Cu mineralization. Their study around porphyry Cu-Mo deposits (3 Mt Cu in total) found that epidote in the immediately surrounding area (up to 1.5 km from the deposit centres) contains low concentrations of light rare earth elements (LREE; < 8 ppm La in most grains), but high abundances of Pb (up to 186 ppm), As (up to 180 ppm), Sb (up to 64ppm), Zr (up to 347 ppm) and Nb (up to 1230 ppm). Epidote enriched in LREE (up to 730 ppm La) occurs farther outside from the deposits, outside the pyrite halo. The data demonstrates that epidote chemistry records a larger footprint of the mineralization than the traditional alteration mineral zoning. Cooke et al. (2014) suggest an exploration method based on the intensity of epidote veining and the modal distribution of this mineral. The use of epidote has also been suggested in exploration for Au deposits by Roache et al. (2011), who demonstrated a positive relationship between the abundance of Fe-rich epidote and the size of Au deposits in Archean greenstone belts in Western Australia. Epidote replaces calcic plagioclase. They also show that the composition of epidote group minerals is correlated with that of co-existing chlorite. Chlorite is a common mineral in a variety of rocks, but the composition of chlorite associated with porphyry-type mineralization appears to be distinct (Wilkinson et al 2015). The data of chlorite may be useful in exploration for porphyry type deposits.

Glacial sediments in the study area contain abundant epidote, apatite, jarosite, magnetite, titanite, rutile, and zircon and their distribution has been documented by the Geological Survey of Canada

researchers in collaboration with the British Columbia Geological Survey (Fig. 1 and see Plouffe et al., 2014; Plouffe and Ferbey, 2015). These minerals are common in mineralized rocks, as well as in barren igneous and metamorphic rocks that are not related to porphyry Cu deposits. The objective of this project is to characterize the composition of resistate minerals associated to porphyry Cu mineralization at Gibraltar and to compare them with those in barren rocks and tills. Ultimately, characterizing the composition of key minerals in till and stream sediments could be used as a fertility indicator vectoring to porphyry Cu mineralization concealed by glacial sediments. This paper reports the occurrence and major element composition of alteration minerals in samples collected in July, 2015 in the Gibraltar mine and the areas immediately surrounding the mine.

Access

The study area is located approximately 60 km north of the town of Williams Lake, and 20 km N-NE of the northeastern shore of McLeese Lake, British Columbia. The study area is accessed by highway 97 and a paved road to the mine. The eastern part of the study area has abundant logging roads, which allow the access to the eastern and northern parts of the Granite Mountain batholith, and country rocks of the batholith. The Beaver Lake Road runs east to connect to the Philemon Lake Road (an old logging road), which leads to the northern part of the Granite Mountain batholith. The Gibraltar quartz diorite and Nicola Group volcanic rocks are exposed along this road. Farther north on the Philemon Lake Road, a foliated tonalite phase of the Granite Mountain batholith is exposed.

Regional geology

The Gibraltar porphyry Cu-Mo deposit is hosted in the Granite Mountain batholith (Fig. 2). The batholith yields U-Pb zircon ages of 217 ± 12 Ma (Bysouth et al., 1995), 215 ± 0.8 Ma (Ash and Riveros, 2001; Ash et al., 1999), and 209.6 ± 6.3 Ma (Oliver et al., 2009). Drummond et al. (1976) reported K-Ar ages of 203 ± 6 and 204 ± 6 Ma on hornblende in leucocratic tonalite. Although the U-Pb zircon ages are overlapping, the age range suggest that this batholith may have formed through multiple intrusions of magmas with similar dioritic compositions.

The batholith is variably deformed and metamorphosed under greenschist facies conditions (Ash et al., 1999b). To the south, it is in fault contact with the Cache Creek Terrane (Figs.1, 2) that mainly consists of Paleozoic to early Mesozoic chemical and siliclastic sedimentary rocks and mafic volcanic rocks (Shannon, 1982).

A debate has taken place as to whether the Granite Mountain batholith belongs to the Paleozoic Cache Creek Terrane or Mesozoic Quesnel Terrane. The close proximity of the batholith with rocks from both terranes and the relatively poor bedrock exposure in the region have contributed to the debate. Since the batholith is in contact with late Paleozoic rocks of the Cache Creek Terrane to the south and east, Drummond et al. (1973, 1976) and Bysouth et al. (1995) suggested that the batholith belongs to the Cache Creek Terrane, with the local limestones, skarns and schists that occur along the southwest margin of the batholith interpreted to be metamorphosed Cache Creek rocks (Drummond et al., 1976; Panteleyev, 1978; Bysouth et al., 1995). On the other hand, Ash et al. (1999a, b) suggested that the Granite Mountain batholith is part of the Mesozoic Quesnel Terrane and that the batholith was faulted against Cache Creek rocks in post-Triassic time. Ductile shear zones and the associated post-mineralization deformation within the Gibraltar deposit would have formed during this tectonic event. Recent mapping by Schiarizza (2014; 2015) demonstrated that the batholith intruded Nicola Group rocks of Quesnel Terrane, confirming that the batholith does not belong to old Cache Creek Terrane.

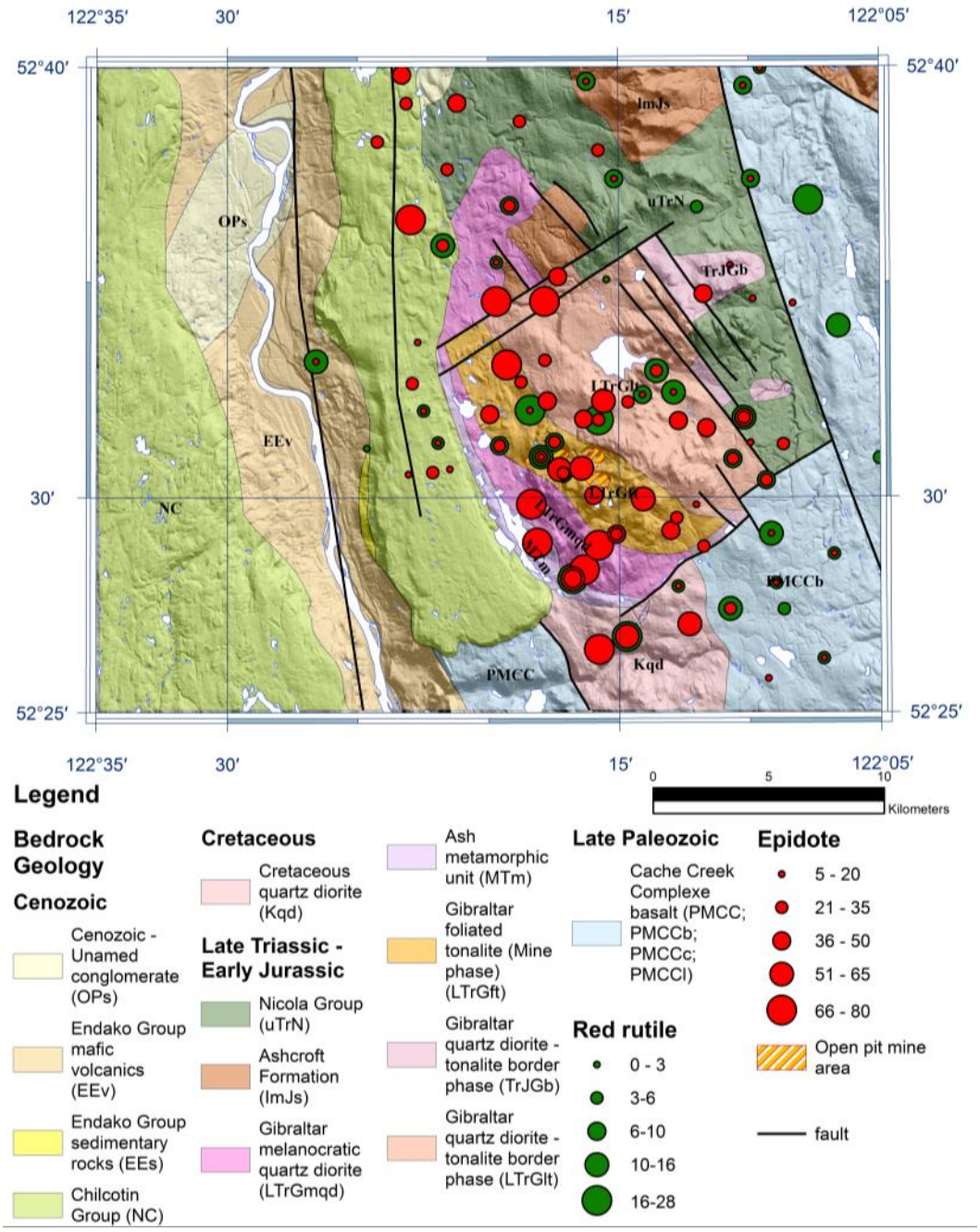

Figure 1. Bedrock geological map and the abundance of epidote and red rutile in tills in the study area. Epidote values are reported as percent of grains of heavy minerals (>3.2 g/cm3) in size fractions ranging from 0.25 to 0.5 mm. Red rutile is reported as the number of grains recovered from 10 kg till samples. Abbreviations, PM: Cache Creek basalt complex, EEs: Endako Group sedimentary rocks. EEv: Endako Group mafic volcanic rocks, Kqd: Cretaceous quartz diorite, LTrGlt: Gibraltar leucocratic tonalite (Granite Mtn phase), LTrGmqd: Gibraltar quartz diorite - tonalite border phase; MTm: Ash metamorphic unit, NC: Chilcotin Group, OPs: Cenozoic sedimentary rocks, TrJGb: Gibraltar tonalite border phase, ImJs: Ashcroft Formation, UtrN: Nichola Group volcanics. (modified after Plouffe et al., 2014).

The volcanic rocks of the Nicola Group are mostly pale green, fine to medium grained tuffs and matrix-supported lapilli tuff breccias of basaltic to andesitic compositions (Schiarizza, 2015). The Nicola Group also contains intercalated siliclastic sedimentary rocks that are dominated by laminated mudstone-siltstone and lesser medium grained volcanic sandstone. These rocks in the proximity to the Granite Mountain batholith show evidence of ductile deformation and similar greenschist metamorphic conditions observed in the batholith.

Conglomerate, sandstone, siltstone and slate present in the north central part of the batholith were originally considered to be the Ashcroft Formation (Logan et al., 2010). More recently, these rocks are correlated to the Dragon Mountain succession which rest unconformably above the Nicola Group (Schiarizza, 2014).

Geology of the Gibraltar deposit

The Gibraltar mine is a Cu-Mo deposit and is the second largest open pit mine in Canada. The mine initially opened in 1972 and processed 36,000 tons/day ore with 0.3 % Cu. In 1996, total geological tonnage (past production plus reserves) of the mine was estimated to be 1,229 Mt ore with 0.3 % Cu (3.69 Mt Cu; Grunsky et al., 1996). It closed in 1999 and reopened in 2004 after realizing the unexploited resource of this deposit. As of 2015, ore extracted from the Gibraltar deposit is estimated to be in excess of 749 Mt at 0.256 wt. % Cu (total 1.92 Mt Cu) and 0.008 wt. % Mo (Taseko Website 2015 http://www.tasekomines.com/gibraltar).

Reserves and Resources of the Gibraltar deposit, December 31, 2014				
	Size (Mt)	Grade (wt%)		Tonnage of Cu (Mt)
		Cu	Mo	
Proven and probable reserves	679.481	0.256	0.008	1.74
Measured & Indicated Resources	990.646	0.254	0.008	2.51

Based on the cut-off of 0.15 wt% Cu (after Jones, 2015).

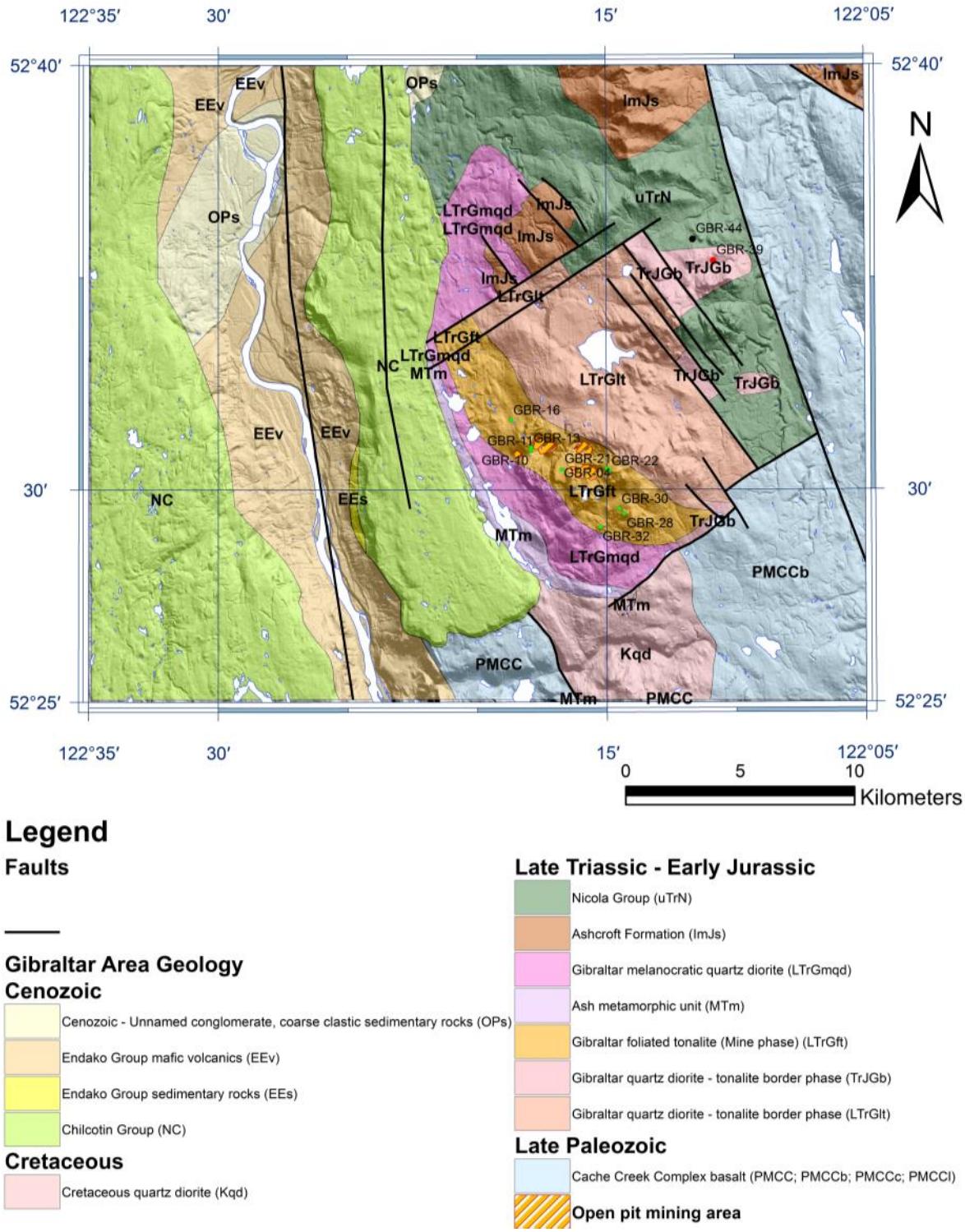

Figure 2. Location map of the Gibraltar Cu-Mo mine and the bedrock geology of the area. Small green circles show the locations of the samples. Bedrock geological map simplified from Ash et al. (1999a), Massey et al. (2005) and Schiarizza (2014).

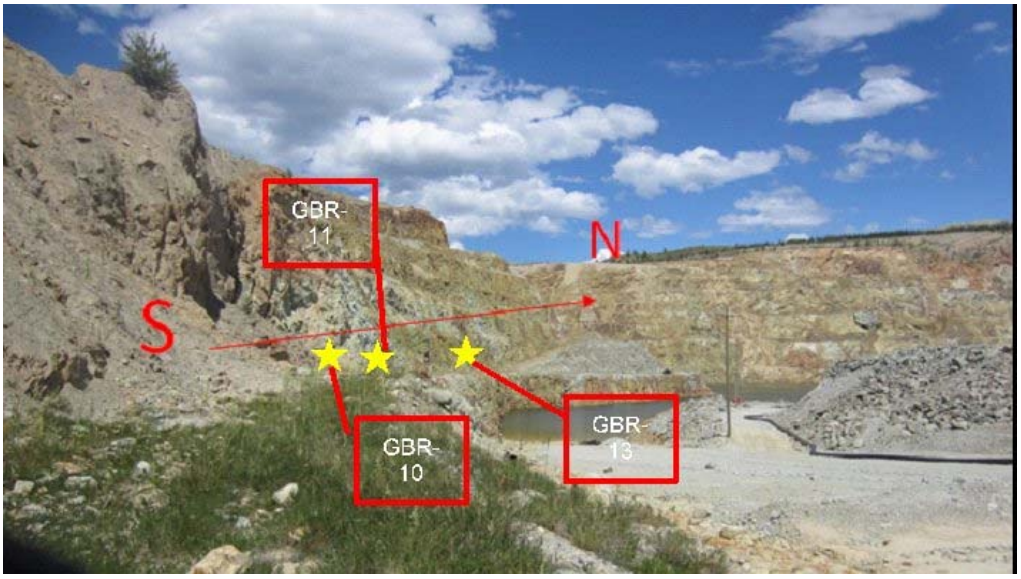

Figure 3. Photograph of the west wall of the East pit at Gibraltar mine, both diorite (GBR-13) and leucocratic tonalite (GBR-11) samples were taken along this traverse including one epidote- and rutile-rich sample (GBR-10). The area is moderately mineralized with visible Cu sulphide minerals and oxidation of sulphides due to weathering from the surface. Epidote appears stable during the weathering and is omnipresent along the traverse. Distances between GBR-10 and -11 and between GBR-11 and GBR-13 are 28 m and 118 m, respectively.

Figure 4. Epidote veining (pointed with a pencil) and dissemination of chlorite-rich aggregates in the leucocratic tonalite phase of Granite Mountain batholith. Sample GBR-30 was collected at this location. Location: Easting 0551505 Northing 5816016 (NAD 83).

Figure 5. Outcrop at sample site GBR-39. Note the wide irregular epidote veining in leucocratic tonalite of the Granite Mountain batholith. Location: Easting 0555489 Northing 5826958 (NAD 83).

Granite Mountain batholith

Lithology and igneous mineralogy

The rocks of the batholith in the area are mostly tonalite (Figs. 3, 4, 5) with minor variation in abundance of quartz, plagioclase and hornblende. Some parts of the batholith are quartz diorite (Fig. 2). Cobaltinitrite staining of saw-cut hand specimens of all samples confirms the absence of K-feldspar phenocrysts in all samples. Porphyritic rocks contain plagioclase phenocrysts (> 5 mm) in a groundmass of fine-grained plagioclase and quartz. Pegmatitic rocks are composed of coarse-crystalline quartz (< 20 mm) and plagioclase (< 20 mm). The igneous mineral assemblage is plagioclase + quartz ± biotite ± hornblende ± apatite ± zircon (Figs. 6 B, C). Epidote appears to be an alteration product, but some coarse-grained crystals and inclusions in plagioclase are possibly magmatic, as magmatic epidote has been reported in tonalitic rocks in many areas (*e.g.,* Schmidt and Poli, 2004; Masumoto et al., 2014).

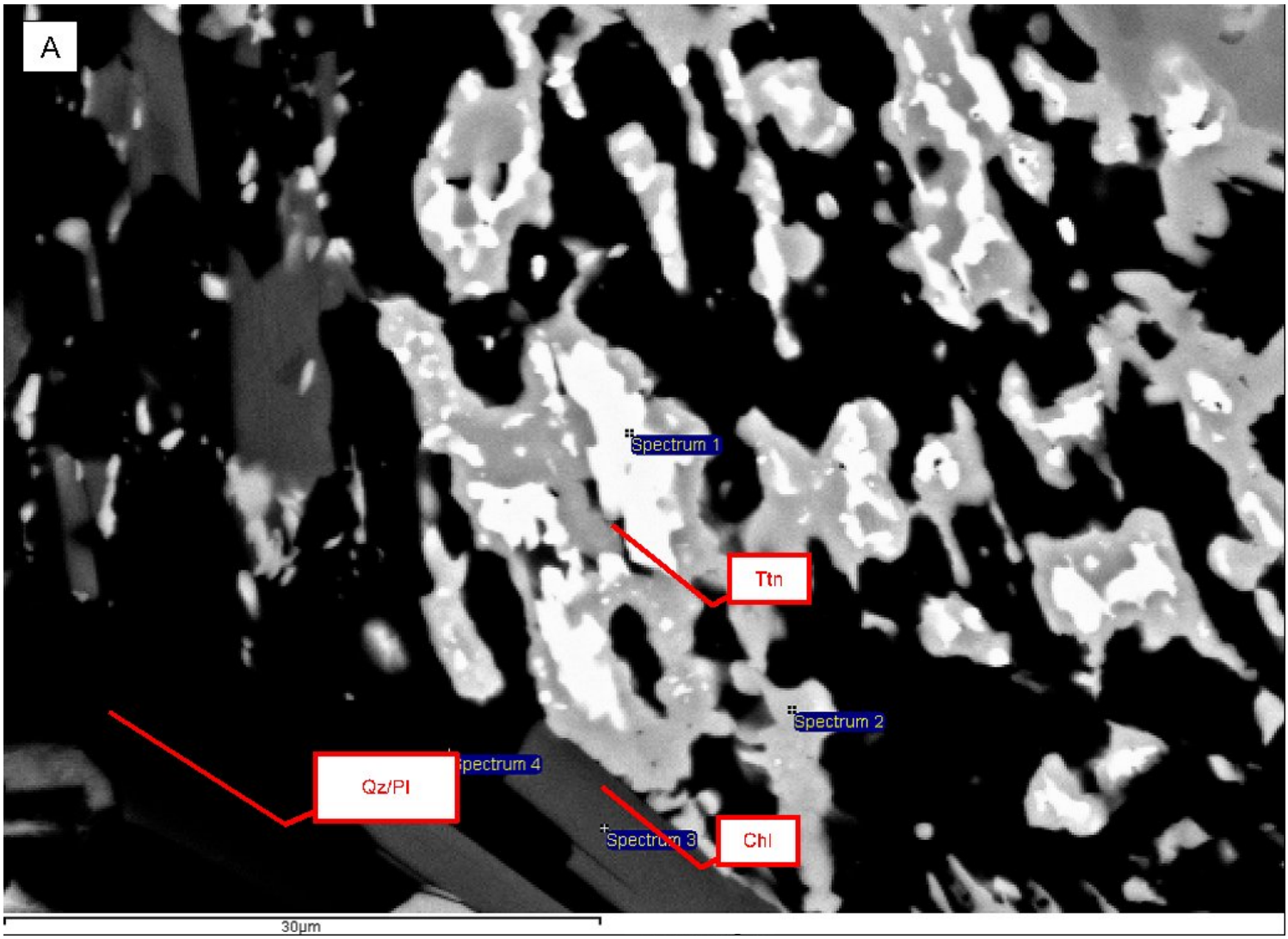
A
Spectrum 1
Ttn
Spectrum 2
Qz/Pl
pectrum 4
Spectrum 3
Chl
30µm

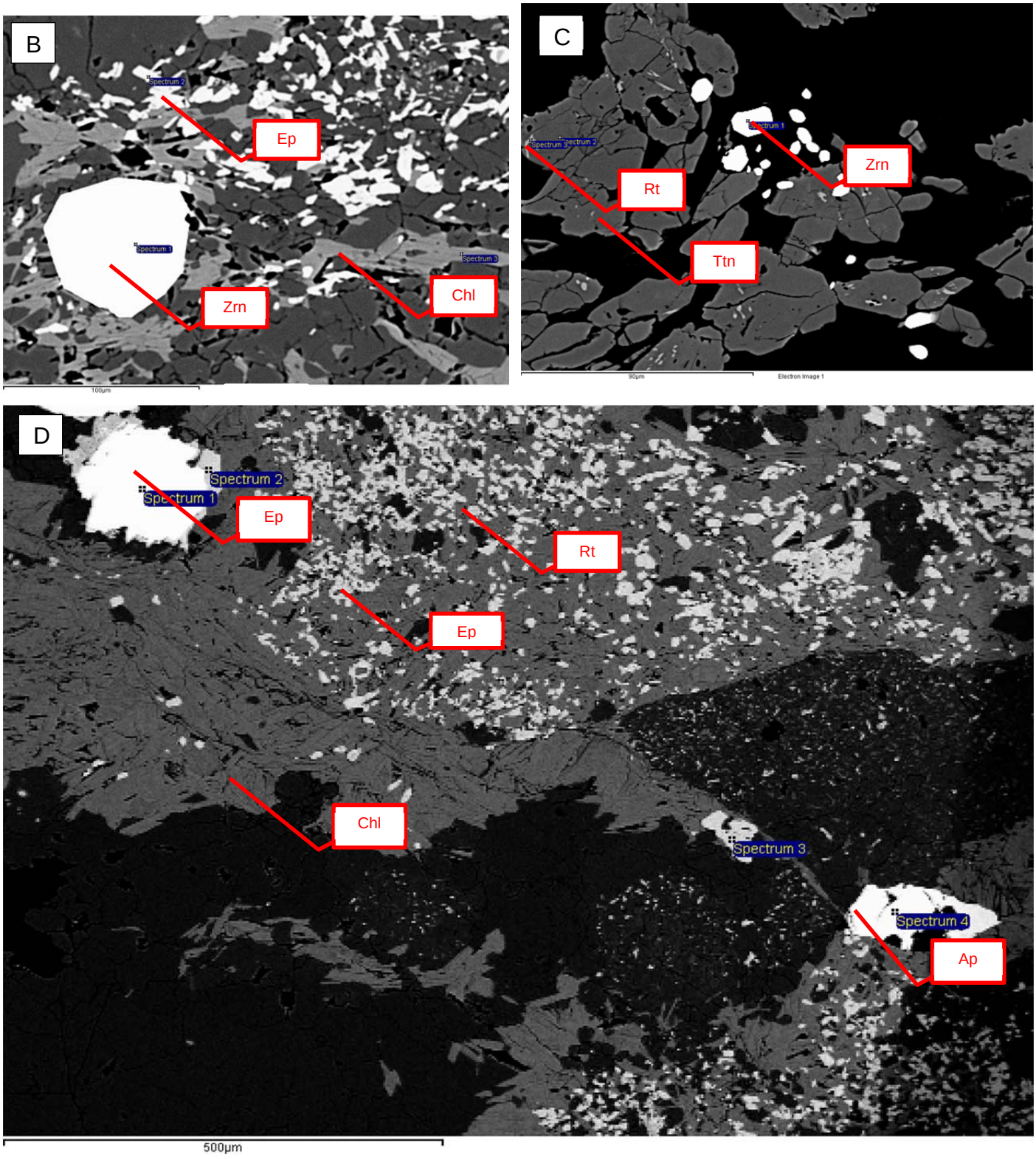
B
Spectrum 2
Ep
Spectrum 1
Zrn
Spectrum 3
Chl
C
Spectrum 1
Spectrum 3
Spectrum 2
Zrn
Rt
Ttn
D
Spectrum 2
Spectrum 1
Ep
Rt
Ep
Chl
Spectrum 3
Spectrum 4
Ap
500µm

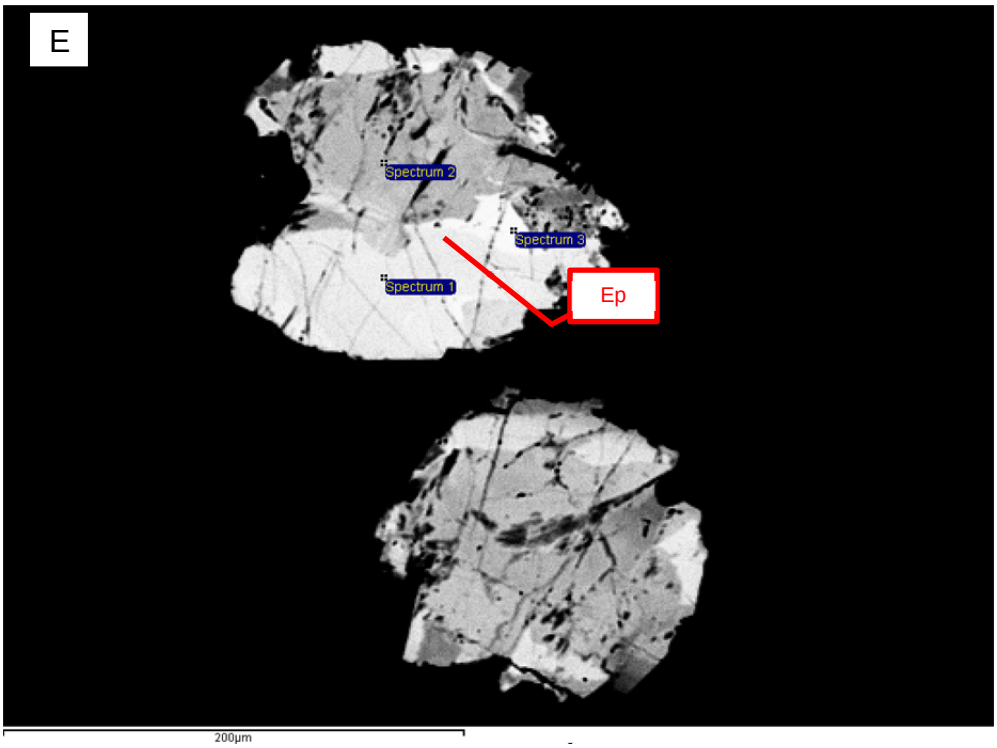
E
Spectrum 2
Spectrum 3
Spectrum 1
Ep
200µm

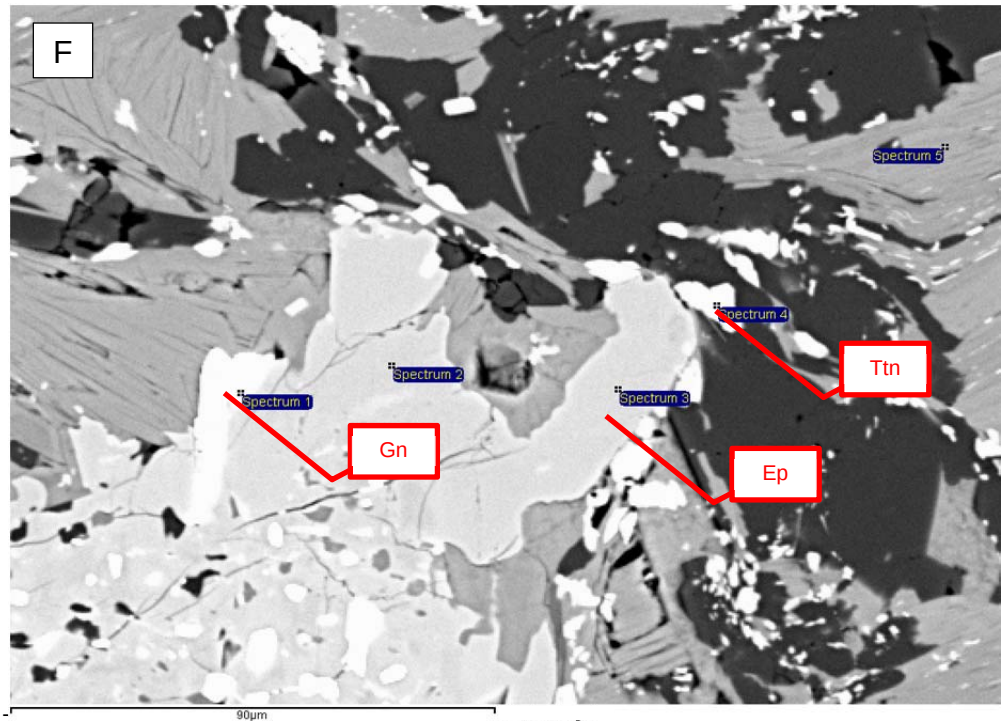
F
Spectrum 5
Spectrum 4
Ttn
Spectrum 2
Spectrum 1
Spectrum 3
Gn
Ep
90µm

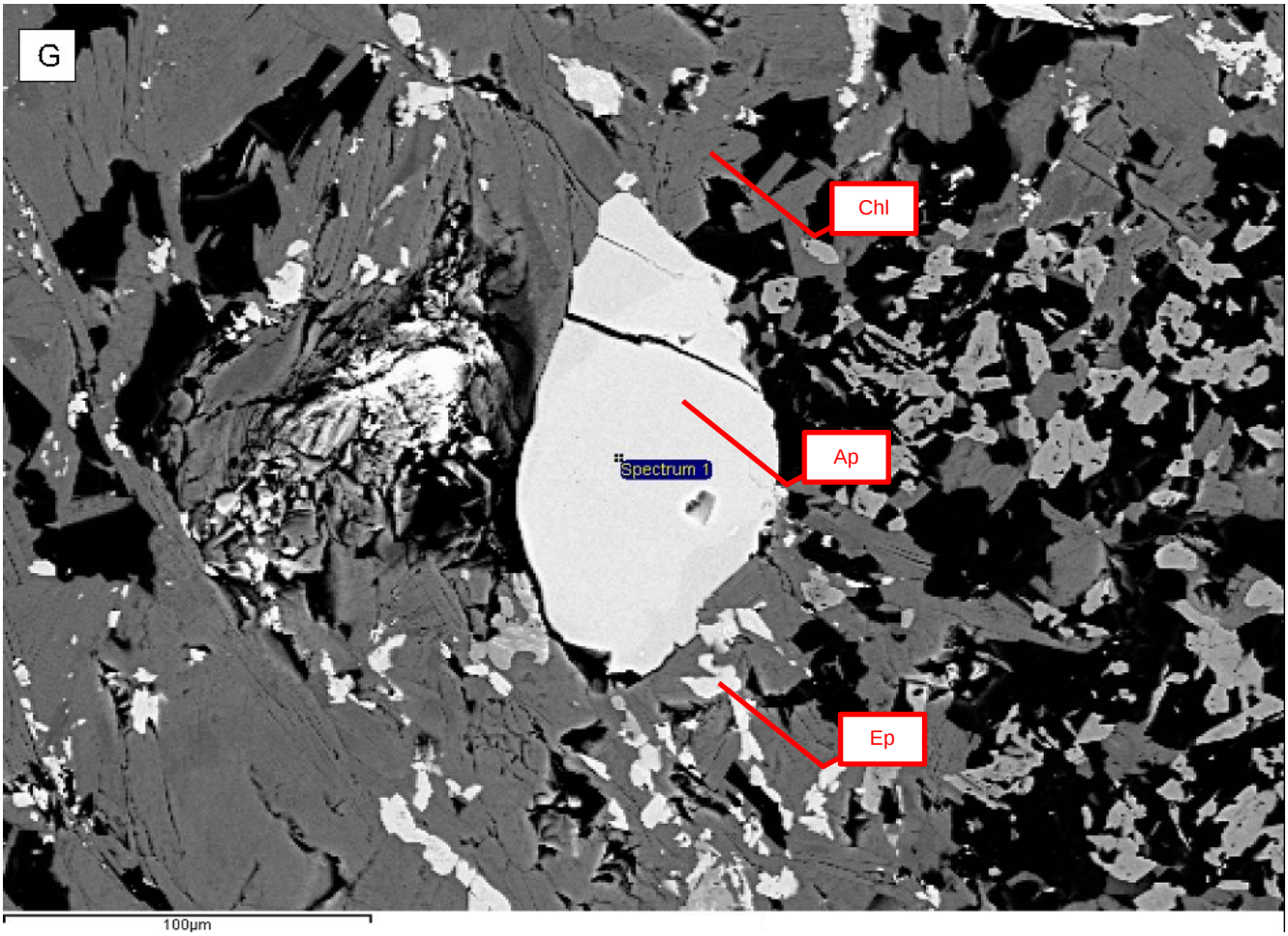

Figure 6. Backscattered electron images showing the common occurrences of titanite, rutile, and epidote. (A) Common occurrence of titanite (Ttn) around rutile (Rt) within aggregates of chlorite. The aggregates are in the groundmass of quartz (Qz) and plagioclase (Pl), Samples GBR-04. (B) epidote (Ep) and zircon (Zrn) in Sample GBR-28, (C) titanite (Ttn), rutile (Rt) and zircon (Zrn) in Sample GBR-16. (D) La- and Ce-rich epidote (Ep) within an aggregate of chlorite (Chl) in the top left and apatite (Ap) bottom right, The epidote contains 6.2 wt %La_2O_3 and 10.6 wt %Ce_2O_3 (Analysis point 6 of Table 1), Sample GBR-28. (E) Compositional zoning of REE-rich epidote (Ep). Greater abundance of La and Ce in brighter parts and the composition is close to the end member component of allanite with 5.04 wt%La_2O_3 and 14.7 wt.% Ce_2O_3. (Analysis point 9 in Table 1). Dark part still contains significant light REE; 5.41 wt.% La_2O_3 and 11.1 wt.% Ce_2O_3 (Analysis point 7 of Table 1), Sample GBR-28. (F) galena (Gn) within an aggregate of chlorite (Chl), epidote (Ep), and titanite (Ttn). Sample GBR-04. (G) a subhedral apatite (Ap) within an aggregate of chlorite (Chl) and epidote (Ep) in Sample GBR-04.

Some samples do not contain hornblende or biotite phenocrysts, but there is the evidence for pseudomorphic replacement of hornblende and biotite by chlorite. Pseudomorphs retain cleavages and crystal habits of the original igneous minerals. Some contain grains of tabular apatite (< 0.5 mm) and euhedral zircon (< 0.5 mm).

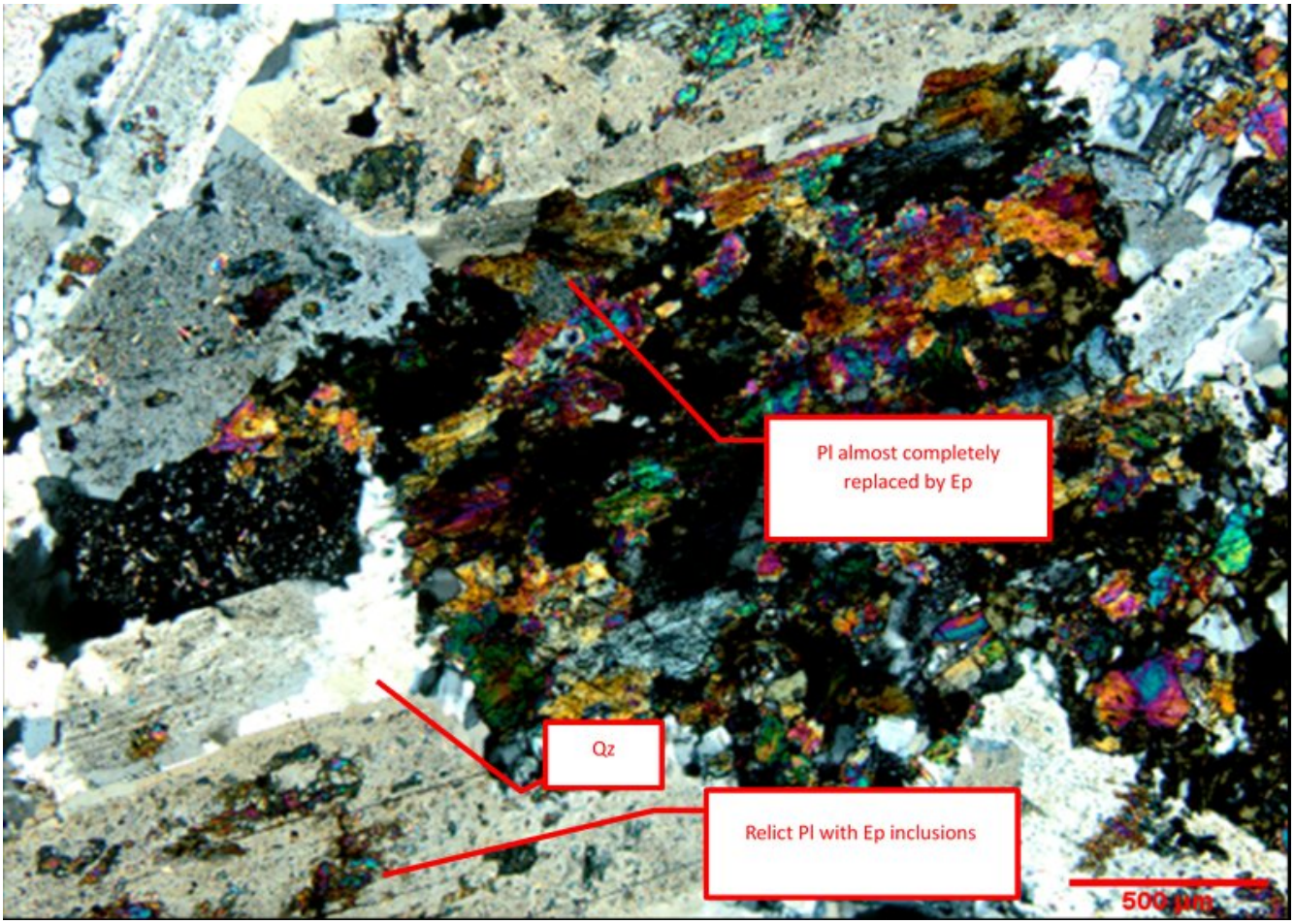

Figure 7. A photomicrograph of the area of plagioclase-rich tonalite (Sample GBR-16) in the thin section shown in Fig. 8C under cross polarized light. The sample GBR-16 was collected along the Gibraltar Mine Road at Easting of 0546717 and Northing of 5819933.

Thin Section Photographs

GBR-10
Easting 0547585, northing 5818572
West wall, East Pit, Gibraltar mine

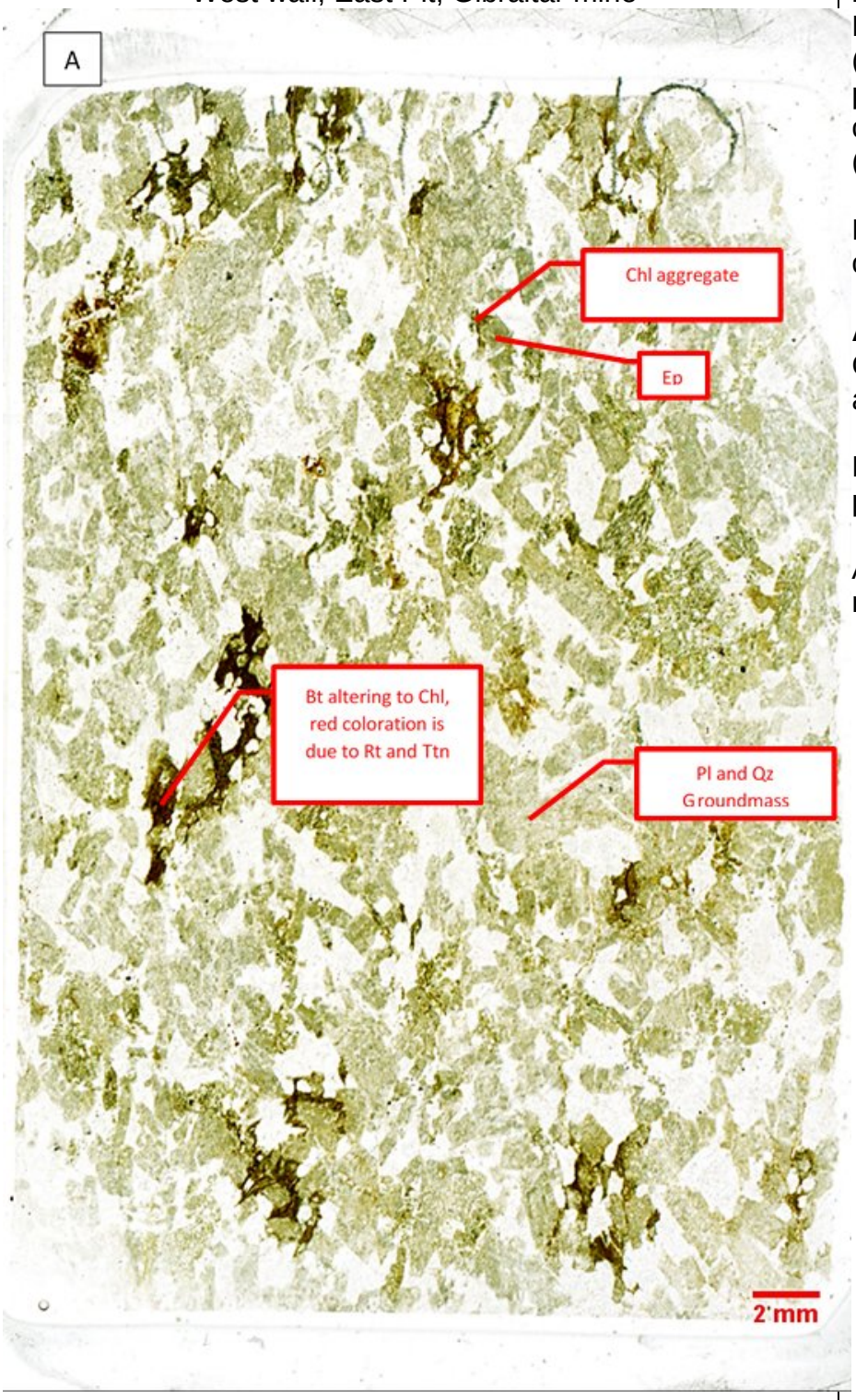

Epidote-rich tonalite

Igneous minerals: Plagioclase (Pl)-quartz (Qz) –biotite (Bt; partially replaced by chlorite (Chl), rutile (Rt) and titanite (Ttn).

Hornblende is not observed

Alteration minerals: Chlorite dissemination and replacing biotite.

Epidote (Ep) within plagioclase crystals.

Apatite or zircon are not observed

GBR-04
Collected at
Easting 0548947, Northing 5817768
West wall, East Pit Gibraltar mine

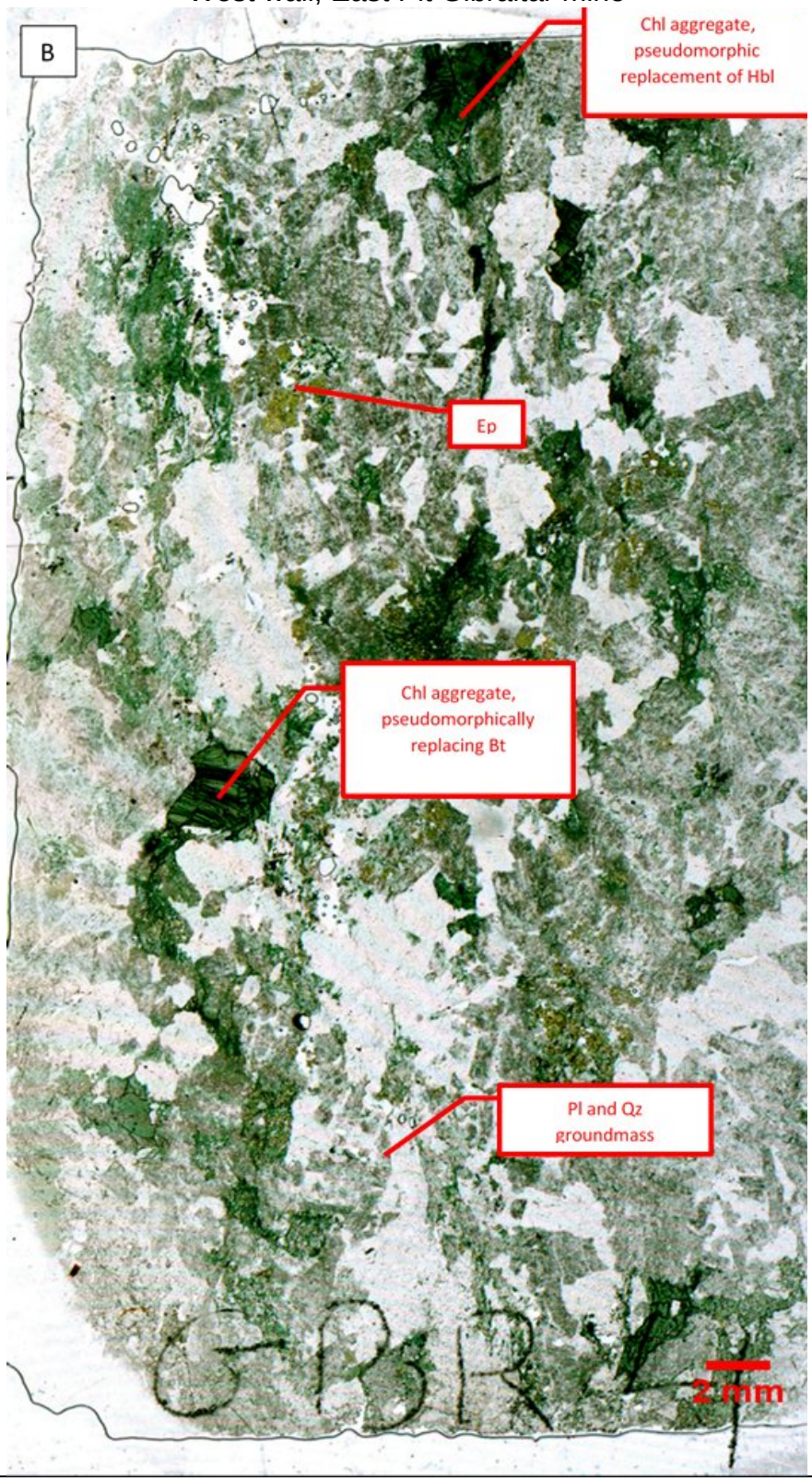

Melanocratic tonalite

Igneous minerals: Plagioclase (Pl)-quartz (Qz)-biotite (altered to chlorite)- Hornblende (Hbl; partially altered to chlorite)

Alteration Minerals: Chlorite (Chl) –epidote (Ep) –titanite (Ttn)

Biotite (Bt) pseudomorphically replaced by chlorite aggregates.

Hornblende (Hbl) pseudomorphically replaced by chlorite aggregates.

GBR-16
Collected at
Easting 0546716, northing 5819933
Gibraltar mine road outcrop

Plagioclase-rich Tonalite

Igneous minerals:
Plagioclase (Pl)-quartz (Qz)

Alteration Minerals:
Epidote (Ep)-chlorite (Chl)-rutile (Rt)-titanite (Ttn)

Plagioclase is partially to totally replaced by epidote. Some plagioclase grains contain epidote inclusions.
More than 10% of all plagioclase is completely replaced by epidote, and the remaining 90% partially replaced or containing epidote inclusions

Figure 8. Photographs of thin sections of samples shown in Fig. 6. They illustrate the igneous assemblage of a plagioclase- rich tonalite in the Granite Mountain batholith. Igneous minerals, such as plagioclase, biotite and hornblende are commonly altered and the relict and their morphologies give an indication of the primary mineralogy. (A) epidote-rich tonalite, Sample GBR-10. (B) melanocratic tonalite, Sample GBR-04. (C) leucocratic tonalite, Sample GBR-16.

Hand sample photographs	Lithology and mineralogy
GBR-10 Easting 0547585, Northing 5818572 West wall, East Pit of the Gibraltar mine 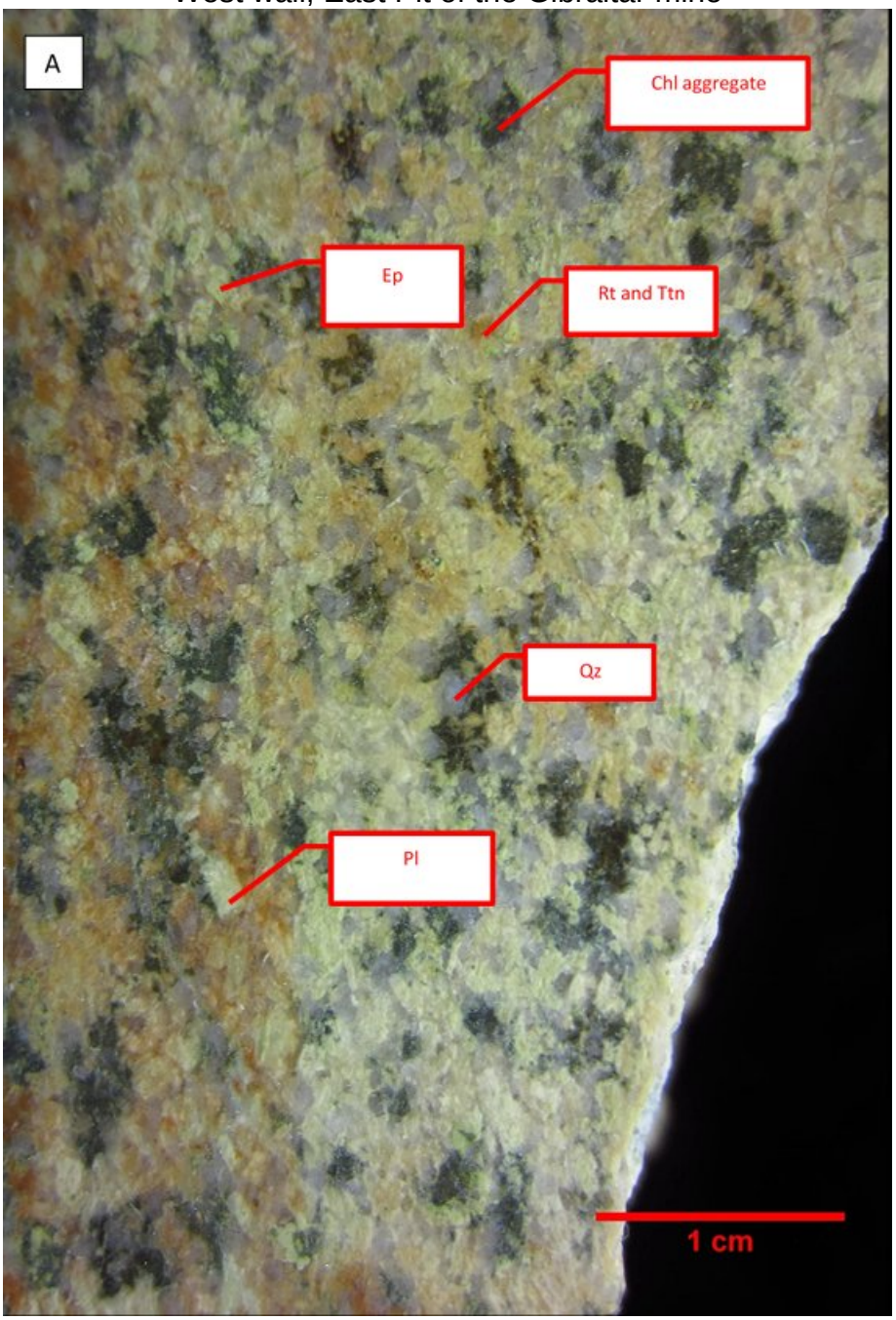 	**Epidote-rich tonalite** **Igneous minerals:** Plagioclase(Pl)-quartz(Qz)- biotite (Bt). Biotite is pseudomorphically replaced by chlorite aggregates. No apatite and zircon grains are observed. **Alteration minerals:** Rutile (Rt) –titanite (Ttn) from biotite. White mica and disseminated epidote (Ep) after plagioclase

GBR-04
Collected at
Easting 0548947, Northing 5817768
West wall, East Pit of the Gibraltar mine

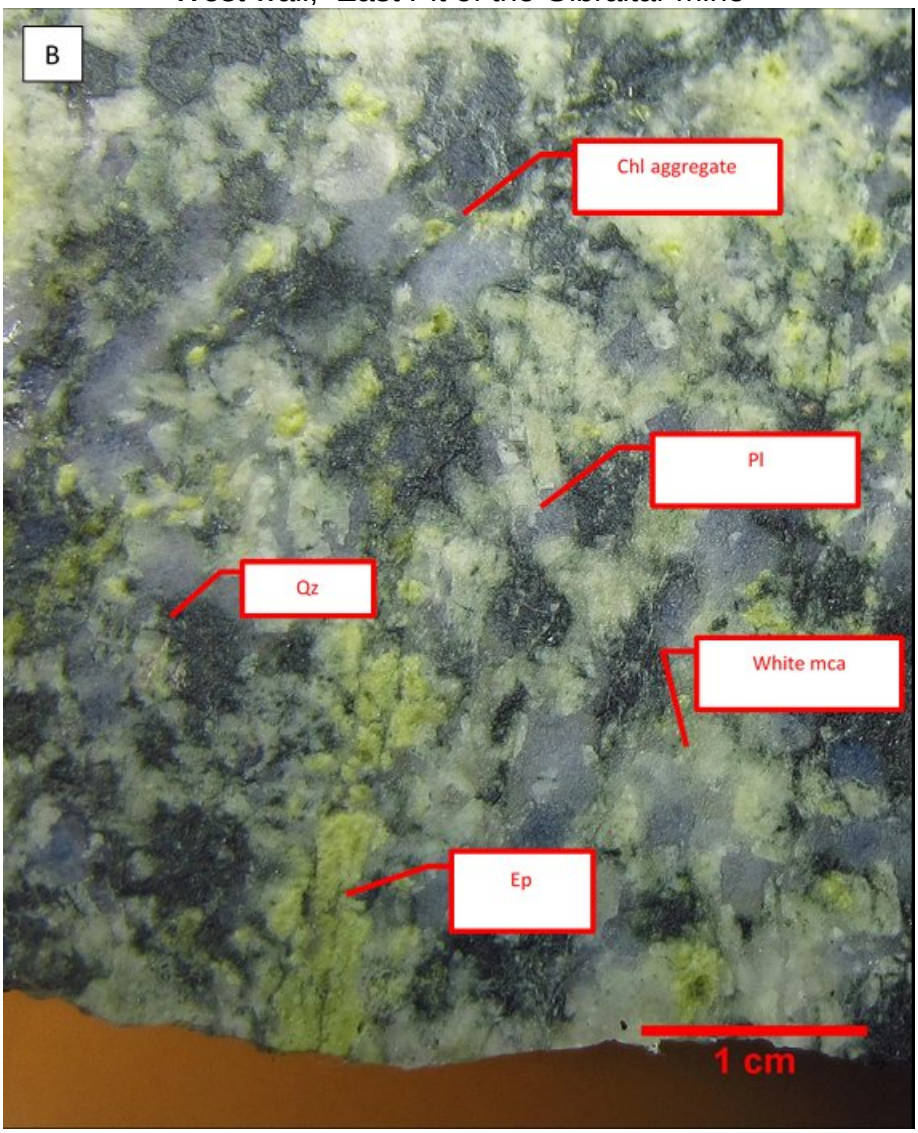

Melanocratic Tonalite

Igneous minerals: Plagioclase (Pl)-quartz (Qz)-Biotite (Bt) and hornblende (Hbl).

Biotite and hornblende pseudomorphically replaced by chlorite (Chl) aggregates.

Apatite and zircon grains are not observed in this sample.

Alteration minerals: Dissemination of white mica (white mca).

Epidote (Ep) and chlorite (Chl) in Qz veinlets

GBR-16
Collected at
Easting 0546716, Northing 5819933
Gibraltar mine road outcrop

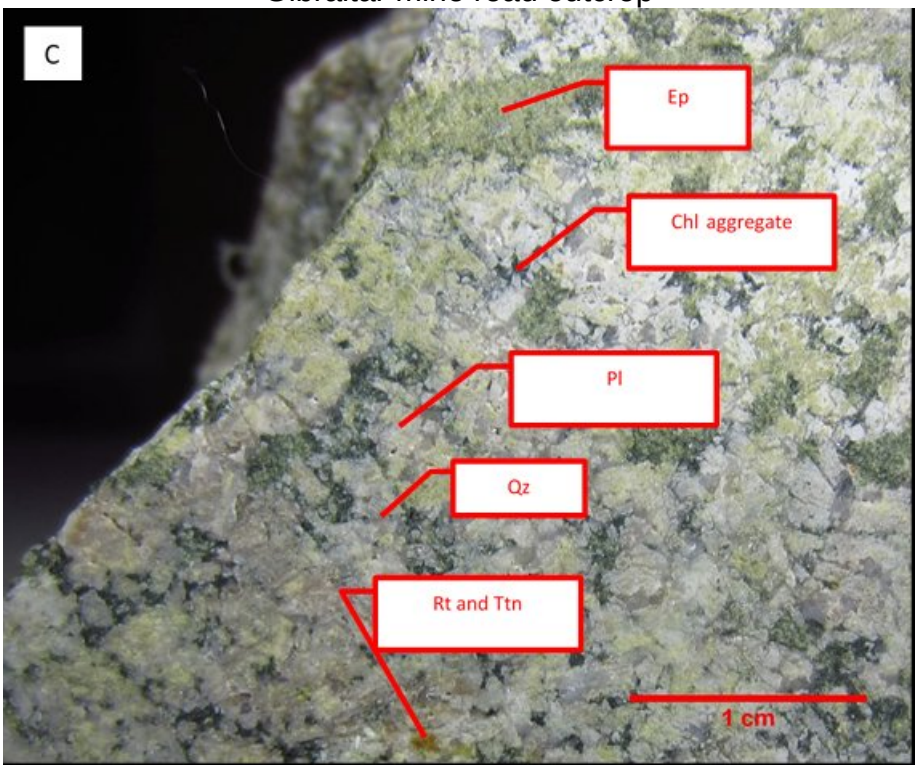

Leucocratic Tonalite

Igneous minerals
Plagioclase (Pl)- quartz (Qz)- biotite or hornblende (now replaced by aggregates of chlorite (Chl).

No apatite or zircon visible at this range

Alteration minerals
Chlorite-white mica-rutile (Rt)- titanite (Ttn)

dissemination of epidote (Ep)

Figure 9. Representative hand sample photographs showing the primary igneous phases and alteration minerals in the tonalitic rock of the Granite Mountain batholith. (A) epidote-rich tonalite, Sample GBR-10. (B) melanocratic tonalite, Sample GBR-04. (C) Leucocratic tonalite, Sample GBR-16.

Methodology

Petrographic studies using plane polarized and cross polarized transmitted and reflected light microscopy was carried out on 13 representative thin sections for this study. Chemical compositions of minerals were determined on 6 carbon-coated polished thin sections using a JEOL 6610LV scanning electron microscope equipped with energy dispersive spectroscopy (SEM-EDS) at the University of Ottawa. Total Fe content is expressed as FeO(t)

Hydrothermal alteration and alteration minerals

Effect of hydrothermal alteration is dependent on the minerals formed during the igneous processes. Some samples (Samples GBR-4, -10, -11, -13, and -22) are intensely altered and most igneous minerals are completely lost (Fig. 7).

Alteration assemblages

Three types of alteration assemblages are recognized. Type 1 contains epidote, chlorite, apatite, magnetite and hematite (Samples GBR-21, -28, -39), Type 2 shows an assemblage of epidote, chlorite, illite, magnetite, titanite and calcite (Sample GBR-30). Type 3 contains an assemblage of epidote, chlorite, illite, titanite, rutile and apatite (Samples GBR-04, -11, -13, -16, and -22).

Alteration is intense along veins containing chlorite, epidote and quartz (Figs. 8B, 9B, 9C). There are mono-minerallic veins of epidote, but most veins are composed of a mixture of epidote, chlorite ± quartz.

Epidote

Epidote with the general formula $A_2M_3[T_2O_7][TO_4](O,F)OH$, has a large compositional variation as the sites of A, M, and T can accommodate a variety of elements. Within epidote supergroup, there are several subgroups and wide solid solution relationships among subgroups. Subgroups include allanite subgroup for epidote with high concentrations of Y and LREE, and piemontite subgroup for Mn-rich variety (Armbruster et al., 2006). In hand specimens and thin sections under transmitted light, all grains in our samples are greenish colour and proper identification of epidote minerals requires quantitative analysis of their compositions. For the purpose of this open file report, all green grass coloured-minerals with optical properties of epidote in hand specimens and thin sections are named epidote including allanite (Figs. 9D, E).

Epidote occurs in all samples from the study area in various degrees of modality (10- 30 vol. %). Epidote shows three types of occurrences. The first type occurs as isolated small (<100 μm) inclusions in plagioclase. Epidote inclusions are all Al-rich (22-25 wt%Al_2O_3) and do not show any compositional zoning in back-scattered electron images. The second type of epidote forms aggregates that are disseminated in rocks and plagioclase phenocrysts. Some plagioclase grains are completely replaced by aggregates of epidote while retaining the original tabular shape of plagioclase (Figs. 7, 8C, 9A, 9B). Colours vary from pistachio green to pale greenish yellow even within individual grains in thin section under transmitted light. They are compositionally zoned with Fe-rich (12-15 wt%FeO (t)) cores and Al-rich rims. The third type of epidote forms mono-minerallic veinlets (up 10 cm in width; Figs. 4, 5). Narrow epidote veinlets are also observed in thin sections. Some veinlets cut through samples and fill fractures of minerals (Fig. 6F). Such veinlets are commonly bordered by narrow (<0.1 mm) bands of chlorite (Fig. 6F). Epidote in the veinlets is Fe-rich (12-15 wt% FeO(t)) with no discernible compositional zoning in back-scattered electron images.

The compositions of twenty four epidote grains were determined with SEM-EDS. Some grains are Al-rich with ≥22.4 wt% Al_2O_3 , close to the end member component of clinozoisite (Figs. 10 A, B). Several grains contain high contents of LREE, up to 9.54 wt % La_2O_3 and 14.7 wt% Ce_2O_3. They are close to the end member composition of allanite (Figs. 10 A, B). These grains have a brown-yellow hue in thin sections. Epidote in the Gibraltar mine pits is all low in LREE (<6 wt% total REE+Y oxides). The LREE-rich epidote occurs >2 km south from the Gibraltar mine pits in Samples GBR-16, -21 and -28 (Figs. 6D, E). The spatial relationship between the occurrences of LREE-bearing epidote and the mineralization in the study area are consistent with the findings by Cooke et al (2014) in the Baguio district of the Philippines, although the absolute concentrations of REE in our samples are

much higher than those of their epidote samples. Cooke et al (2014) reported low concentrations of LREE in epidote close to the mineralized areas and elevated concentrations of LREE (up to 1487 ppm La) in epidote farther outside the area surrounding the mineralization.

Table 1. Major element abundances of epidote expressed in wt % determined with SEM-EDS.

Sample	Grain #	Na_2O	MgO	Al_2O_3	SiO_2	CaO	TiO_2	MnO	FeO(t)*	Sc_2O_3	Ce_2O_3	La_2O_3
GBR-11	1	<0.1	<0.1	25.3	39.7	23.5	0.4	0.7	10.5	0.0	<0.1	<0.1
GBR-11	2	<0.1	<0.1	22.5	38.4	21.6	0.3	0.4	11.2	2.2	<0.1	<0.1
GBR-11	3	<0.1	<0.1	24.9	39.2	23.6	<0.1	0.6	11.4	0.3	<0.1	<0.1
GBR-32	4	<0.1	<0.1	24.5	39.9	23.6	<0.1	0.5	11.4	0.0	<0.1	<0.1
GBR-11	5	<0.1	<0.1	23.9	39.6	22.3	<0.1	1.0	11.6	0.8	<0.1	<0.1
GBR-11	6	<0.1	<0.1	22.6	39.0	23.6	0.5	0.3	11.6	2.5	<0.1	<0.1
GBR-11	7	<0.1	<0.1	22.4	38.4	22.0	0.4	0.5	11.8	2.0	<0.1	<0.1
GBR-32	8	<0.1	<0.1	24.4	40.1	23.0	<0.1	<0.1	12.4	0.0	<0.1	<0.1
GBR-32	9	1.7	<0.1	22.5	42.5	20.8	<0.1	<0.1	12.5	<0.1	<0.1	<0.1
GBR-04	10	<0.1	<0.1	23.9	39.6	23.4	0.2	<0.1	12.9	<0.1	<0.1	<0.1
GBR-21	11	<0.1	<0.1	22.1	38.3	17.1	<0.1	<0.1	12.9	<0.1	5.6	<0.1
GBR-04	12	<0.1	<0.1	23.7	39.3	23.9	<0.1	<0.1	13.1	<0.1	<0.1	<0.1
GBR-28	13	<0.1	<0.1	23.6	39.5	23.3	<0.1	0.4	13.1	<0.1	<0.1	<0.1
GBR-28	14	<0.1	<0.1	23.7	39.2	23.2	<0.1	0.5	13.3	<0.1	<0.1	<0.1
GBR-04	15	<0.1	<0.1	22.9	39.4	23.6	<0.1	<0.1	13.7	<0.1	<0.1	<0.1
GBR-11	16	<0.1	<0.1	22.7	39.5	23.4	0.6	<0.1	13.7	<0.1	<0.1	<0.1
GBR-21	17	<0.1	<0.1	22.9	38.9	23.9	0.0	<0.1	14.4	<0.1	<0.1	<0.1
GBR-32	18	<0.1	<0.1	22.2	38.9	23.9	0.3	<0.1	14.7	<0.1	<0.1	<0.1
GBR-21	19	<0.1	<0.1	22.2	39.9	23.0	<0.1	<0.1	15.0	<0.1	<0.1	<0.1
GBR-11	20	<0.1	<0.1	22.1	39.3	23.1	<0.1	<0.1	15.5	<0.1	<0.1	<0.1
GBR-11	21	<0.1	<0.1	21.7	38.8	23.6	<0.1	0.2	15.6	<0.1	<0.1	<0.1
GBR-28	22	0.9	<0.1	15.9	34.4	14.2	<0.1	0.9	17.5	<0.1	10.1	6.2
GBR-28	23	<0.1	1.0	15.4	34.7	13.9	<0.1	0.9	17.5	<0.1	11.1	5.4
GBR-28	24	<0.1	1.3	13.1	33.7	11.8	<0.1	1.0	18.5	<0.1	11.1	9.5
GBR-28	25	<0.1	1.6	12.5	34.3	11.5	<0.1	1.0	19.4	<0.1	14.7	5.0

*Total Fe expressed as FeO(t)

The concentration values are based on the sum of anhydrous components to be 100 %.

Description of analysed areas:

1= Outer darker rim of zoned grain (back scatter image), surrounded by other unzoned epidote grains within a chlorite and epidote rich quartz vein.

2= zoned epidote grain (inner brighter core (back scatter image), surrounded by other epidote grains (unzoned), within a chlorite and epidote rich quartz rich vein.

3= zoned epidote grain (outer darker rim, back scatter image), surrounded by other epidote grains (unzoned), within a chlorite and epidote rich quartz vein.

4= zoned epidote grain (inner brighter core, back scatter image), surrounded by other epidote grains (unzoned), within a chlorite and epidote rich quartz rich vein.

5= zoned epidote grain (inner brighter core, back scatter image), surrounded by other epidote grains (unzoned), within a chlorite and epidote rich quartz rich vein.

6= Unzoned epidote grain, in contact with darker epidote grains (back scatter image) with no detectable REEs and chlorite and quartz.

7= Zoned epidote grained (darker part, back scatter image) in contact with quartz grains.

8= Zoned epidote grained (brighter part, back scatter image) in contact with quartz grains.

9= Zoned epidote grained (brightest part, back scatter image) in contact with quartz grains.

10=Unzoned epidote grain in contact with titanite grain within chlorite aggregate.

11= Zoned epidote grain (inner brighter core, back scatter image), surrounded by other epidote grains (unzoned), within a chlorite and epidote rich quartz rich vein.

12= Unzoned tabular epidote grain in contact with plagioclase grains and chlorite grains.

13= Elongate epidote grain within a relict plagioclase grain.

14= Unzoned epidote grain in contact with plagioclase and chlorite within a chlorite aggregate.

15= Small epidote grain (<0.5um long) surrounded by chlorite in a quartz/chlorite vein.

16= Unzoned epidote grain in contact with chlorite within a chlorite aggregate.

17= Unzoned isolated epidote grain surrounded by chlorite in a large chlorite aggregate (1mm across).

18= Unzoned epidote on the fringe of a larger Ce/La rich epidote grain in contact with chlorite in a chlorite aggregate.

19= Unzoned epidote grain in contact with quartz and plagioclase grains.

20= Unzoned epidote grain in contact with plagioclase and chlorite grains within a chlorite aggregate.

21= Unzoned epidote grain in contact with plagioclase and other epidote grains in an epidote aggregate.

22= Unzoned elongate epidote grain within a relict plagioclase grain.

23= Unzoned elongate epidote grain within a relict plagioclase grain.

24= Unzoned epidote grain surrounded by chlorite, in a chlorite rich aggregate that contains titanite.

25= Unzoned epidote grain surrounded by chlorite in a chlorite/epidote aggregate. This agreagate contains zoned epidote grains in its center.

Titanite

Titanite has two origins; a discrete micro-phenocryst of igneous origin and an alteration product. Two types of titanite show distinctly different crystal habits, optical properties and compositions. Igneous titanite contains lower Al_2O_3 (1.20- 1.21 wt. %) whereas hydrothermal titanite contain high Al_2O_3 ranging from 2 to 6 wt. % (Fig. 10C).

Igneous titanite forms euhedral tabular crystals (>1 mm long and >0.3 mm wide), shows brown hue with high relief in thin sections under transmitted light. Igneous titanite is observed in samples GBR-13, -16, and -22. Hydrothermal titanite is observed in most samples within the aggregates of chlorite and epidote, and in chlorite-quartz veins. It forms needles (<50 μm in length, <10 μm in width; Figs. 8, 9A). Hydrothermal titanite is almost opaque in thin sections under transmitted light.

Table 2. Major element concentrations of titanite in wt %

Sample	Grain#	Na_2O	MgO	Al_2O_3	SiO_2	CaO	V_2O_3	TiO_2	MnO	FeO(t)*
Alteration Titanite										
GBR-32	1	1.18	<0.1	5.72	36.7	23.4	<0.1	31.2	<0.1	1.9
GBR-11	2	<0.1	<0.1	4.99	32	28.6	<0.1	32.7	<0.1	1.8
GBR-21	3	<0.1	0.96	4.95	31.6	25.9	1.05	32.7	<0.1	2.9
GBR-04	4	<0.1	0.56	5.4	31.5	27.5	<0.1	33.2	<0.1	1.9
GBR-11	5	<0.1	3.13	5.1	30.3	23.5	<0.1	33.6	<0.1	4.4
GBR-04	6	<0.1	<0.1	4.92	31.6	28.3	<0.1	34.2	<0.1	0.9
GBR-28	7	<0.1	<0.1	1.14	39.5	23.4	<0.1	34.4	<0.1	1.5
GBR-04	8	<0.1	0.57	5.76	29.9	27.2	<0.1	34.9	<0.1	1.6
GBR-21	9	<0.1	<0.1	4.08	31.3	28.4	<0.1	35.7	<0.1	0.5
GBR-11	10	<0.1	1.14	3.04	31.7	26.1	<0.1	36	0.22	1.8
GBR-32	11	<0.1	0.6	1.92	31.8	27.2	<0.1	36.6	<0.1	1.9
GBR-32	12	<0.1	<0.1	2.6	31.2	28.2	<0.1	37	<0.1	0.9
GBR-11	13	<0.1	<0.1	3.09	30.9	26.6	<0.1	37.7	<0.1	1.7
GBR-11	14	<0.1	<0.1	3.23	30.6	26.4	<0.1	37.7	<0.1	2.1
GBR-11	15	<0.1	<0.1	2.24	30.9	27.7	<0.1	38.1	<0.1	1.0
GBR-11	16	<0.1	<0.1	2.03	31.0	27.6	<0.1	38.2	<0.1	1.1
GBR-32	17	<0.1	<0.1	1.78	30.8	28.3	<0.1	38.3	<0.1	0.8
GBR-11	18	<0.1	<0.1	1.4	32.2	26.6	<0.1	38.3	<0.1	1.5
GBR-04	19	<0.1	0.41	3	31	25.6	<0.1	38.5	<0.1	1.6
Igneous Titanite										
GBR-28	20	<0.1	<0.1	1.3	30.9	27.1	<0.1	38.7	<0.1	1.9
GBR-28	21	<0.1	<0.1	1.2	30.1	27.7	<0.1	38.7	<0.1	2.4
GBR-16	22	<0.1	<0.1	1.3	30.3	27	<0.1	38.8	<0.1	1.8
GBR-16	23	<0.1	<0.1	1.6	31.0	28.1	<0.1	38.8	<0.1	0.5
GBR-11	24	<0.1	<0.1	1.5	31.9	26.5	<0.1	38.9	<0.1	1.1
GBR-16	25	<0.1	<0.1	1.2	30.6	27.6	<0.1	39.1	<0.1	1.5
GBR-16	26	<0.1	<0.1	1.2	30.7	27.2	<0.1	39.5	<0.1	1.4

**Total Fe expressed as FeO (t)*

1= elongate grain in contact with quartz and chlorite grains, 2= isolated grain in contact with chlorite grains within a chlorite-epidote-rich quartz vein, 3= elongate grain within a titanite aggregate in contact with chlorite grains, 4= tabular grain within a titanite aggregate in contact with other grains and rutile gains, 5= isolated grain surrounded by chlorite grains within a quartz vein, 6= isolate grain in contact with quartz and epidote within a chlorite-epidote rich quartz vein, 7= grain fracture filling fractures in a quartz grain, 8= Titanite grain within the centre of a chlorite aggregate within a quartz vein, in contact with rutile in the centre of the grain, 9= subhedral grain within a chlorite aggregate in a quartz veins, 10= isolated grain surrounded by chlorite grains within a quartz vein, 11= isolated grain surrounded by chlorite grains within a quartz vein, 12= isolated grain surrounded by chlorite grains within a quartz vein, 13= subhedral grain in the centre of a chlorite aggregate in a quartz vein, 14= subhedral grain in the centre of a chlorite aggregate in a quartz vein, 15= subhedral grain in the centre of a chlorite aggregate in a quartz vein, 16= subhedral grain in the centre of a chlorite aggregate in a quartz vein, 17= subhedral grain in contact with epidote and chlorite, 18= isolated grain surrounded by chlorite grains within a quartz vein, 19= grain in contact with quartz containing rutile in its centre, 20= large euhedral titanite (<100 µm) in contact with quartz, 21= large euhedral titanite (<400 µm) in contact with quartz, 22= large euhedral titanite (<400 µm) in contact with quartz, 23= Small euhedral grain in contact with quartz and titanite, 24= subhedral grain with chalcopyrite and pyrite inclusions in contact with quartz and chlorite, 25= large euhedral grain (600 µm) surrounded by plagioclase and quartz, 26= large euhedral grain (600 µm) surrounded by plagioclase and quartz

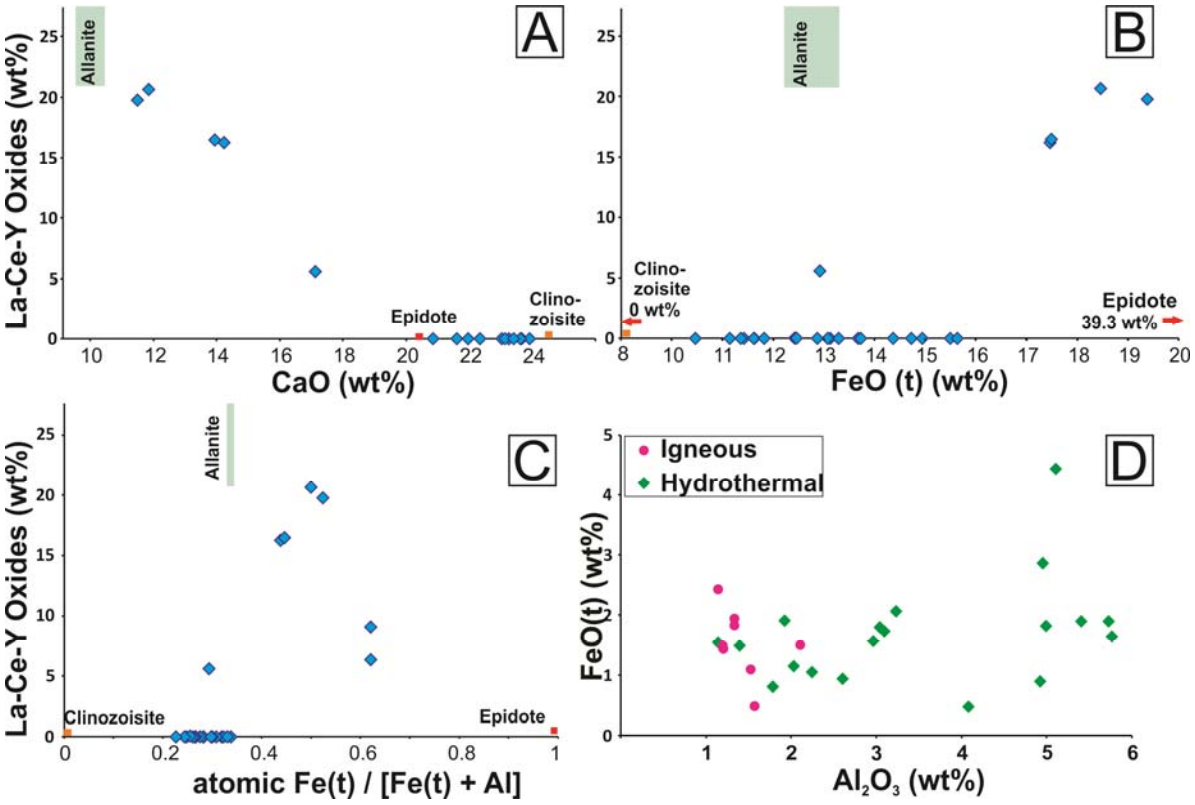

Figure 10. Binary plots of major element compositions of epidote (A,B,C) and titanite (D) in the samples. They show the end member components of epidote ($Ca_2Fe^{III}_3(SiO_4)_3(OH)$), clinozoisite $Ca_2Al_3(SiO_4)_3(OH)$, and allanite $CaMAl_2Fe^{II}(SiO_4)_3(OH)$ where M is La, Ce or Y.

Rutile

Rutile in the samples is an alteration product, and commonly associated with biotite. Rutile occurs with titanite in the aggregates of chlorite and epidote, and in chlorite-epidote veins as small elongated

crystals (<20 μm in length) within titanite aggregates in most cases. Rutile grains are opaque in thin sections under transmitted light and are disseminated within dark brown to opaque aggregates of titanite (Fig. 6 A). This occurrence makes it difficult to observe red coloration of rutile in thin sections. Large (approx. 0.2 mm long and <0.1mm wide), subhedral and red-coloured rutile crystals have been observed in chlorite and epidote aggregates in 3 samples (GBR-10, -16, and -28). Rutile contains minor Al_2O_3 (up to 0.3 wt.%) and CaO (up to 3.7 wt.%).

Table 3. Major element concentrations of rutile expressed in wt. %

Sample	Grain #	Al_2O_3	SiO_2	CaO	TiO_2	FeO (t)*
GBR-04	1	0.3	1.4	1.2	96.5	0.5
GBR-04	2	0.3	0.3	0.9	97.7	0.9
GBR-04	3	0.2	1.8	1.6	95.8	0.6
GBR-16	4	<0.1	3.6	3.7	92.4	0.4

**Total Fe expressed as FeO (t).*

1= Grain in the centre of a titanite grain within a quartz vein, 2= Grain in the centre of a titanite grain within a chlorite aggregate in a quartz vein, 3= Grain in the centre of a titanite grain within a chlorite aggregate in a quartz vein, 4= Grain in the centre of a titanite grain within a quartz vein

Apatite

Apatite occurs as an alteration mineral in most samples (GBR-04,-10,-11,-13,-16,-21,-22,-30, and -32) and shows the typical bluish grey colour in thin sections under crossed polarizers. It occurs within epidote-rich aggregates, relict plagioclase and the groundmass with plagioclase and quartz. Crystals are up to 100 μm in length and are typically subhedral to anhedral (Fig. 6 G). Apatite grains in Samples GBR-04, -13, -16, -28 and -30, are most likely primary igneous, as they occur as isolated euhedral crystal of approimately 100 μm long and 50 μm wide and away from veins and intensely altered areas of samples. SEM-EDS analysis shows that apatite has a wide compositional variation. All grains have compositions close to the ideal formulae of apatite. Several grains in Sample GBR-21 contain up to 0.4 wt. % MnO, which makes Mn/Ca molar ratios up to 0.006.

Table 4. Apatite compositions expressed in wt %

Sample	Grain #	SiO_2	CaO	MnO	FeO(t)*	P_2O_5
GBR-04	1	<0.1	55.8	<0.1	0	44.2
GBR-11	2	<0.1	55.1	<0.1	0.2	43.9
GBR-21	3	0.9	54.1	0.4	0.3	44.3
GBR-21	4	1.0	54.4	0.4	<0.1	44.2
GBR-28	5	1.0	55.4	<0.1	<0.1	43.7

**Total Fe expressed as FeO (t)*

1= large subhedral grain (100 μm in length) in a chlorite aggregate within a epidote quartz vein, 2= large subhedral grain (100 μm in length) in a chlorite-epidote aggregate, 3= small grain (<50 μm) surrounded by chlorite, 4= small isolate grain (<30 μm) surrounded by quartz, 5= large euhedral grain (250 μm in length) in contact with chlorite and epidote altered plagioclase

Apatite composition in till and bedrock near porphyry deposits of British Columbia was also studied by Rukhlov et al. (2016) and Bouzari et al. (2011).

Summary

This study shows an alteration assemblage of epidote, chlorite, rutile, titanite ± magnetite, ± hematite, ± apatite associated with the Gibraltar porphyry Cu-Mo deposits. Among these alteration minerals, epidote is ubiquitous throughout the Granite Mountain batholith.

Preliminary analyses of the compositions of epidote, titanite, and rutile show very large variations. Some epidote grains contain more than 10 wt.% Ce_2O_3 and more than 5 wt.% La_2O_3, close to the end member component of allanite. Based on a comparison with the reported epidote composition near porphyry mineralization, the Ce and La enrichment in epidote at Gibraltar could be a diagnostic feature of epidote associated with mineralization.

Acknowledgements

Jeffrey Hedenquist is thanked for his help during the field work in July 2015. The project was supported by Discovery Grant from Natural Science and Engineering Council of Canada to KH. This project is part of the M.Sc. thesis of C.K. Neil Rogers completed the internal GSC review. ESS Contribution number 20150489.

References

Armbruster, T., Bonazzi, P., Akasaka, M., Bermanec, V., Chpin, C., Giere, R., Heuss-Assbichler, S., Liebscher, A., Menchetti, S., Pan, Y., and Pasero, M., 2006. Recommended nomenclature of epidote-group minerals; European Journal of Mineralogy, v. 18, p. 551-567.

Ash, C.H., Panteleyev, A., MacLellan, K.L., Payne, C.W., and Rydman, M.O., 1999a. Geology of the Gibraltar Mine area (93B/6&9); British Columbia Ministry of Energy and Mines; Open File 1999-7, scale 1:50 000.

Ash, C.H., Rydman, M.O., Payne, C.W., and Panteleyev, A., 1999b. Geological setting of the Gibraltar mine south central British Columbia (93B/8, 9); *in* Exploration and Mining in British Columbia 1998, British Columbia Ministry of Energy and Mines, p. A1-A15.

Ash, C.H., and Riveros, C.P., 2001. Geology of the Gibraltar copper-molybdenite deposit, east-central British Columbia (93B/9); *in* Geological Fieldwork 2000, British Columbia Ministry of Energy and Mines, Paper 2001-1, p. 119-134.

Bouzari, F., Hart, C.J.R., Barker, S., and Bissig, T., 2011. Porphyry indicator minerals (PIMS): a new exploration tool for concealed deposits in south-central British Columbia; Geoscience BC Report 2011-17, 31 p.

Bysouth, G.D., Campbell, K.V., Barker, G.E., and Gagnier, G.K., 1995. Tonalite-trondhjemite fractionation of a peraluminous magma and the formation of syntectonic porphyry Cu mineralization, Gibraltar mine, central British Columbia; *in* Porphyry Deposits of the Northwestern Cordillera of North America, (ed.) T.G. Schroeter; Canadian Institute of Mining, Metallurgy and Petroleum, Special Volume 46, p. 201–213.

Cooke, D.R., Baker, M., Hollings, P., Sweet, G., Chang, Z., Danyushevsky, L., Gilbert, S. Zhou, T., White, N.C., Gemmell, J.B., and Inglis, S., 2014. New advances in detecting the distal geochemical foot prints of porphyry systems-epidote mineral chemistry as a tool for vectoring and fertility assessments; Economic Geology Special Publication, v.18, p. 127-152.

Drummond, A.D., Tennant, S.J., and Young, R.J., 1973. The interrelationship of regional metamorphism, hydrothermal alteration and mineralization at the Gibraltar mines copper deposit in B.C.; Canadian Mining and Metallurgical Bulletin, v. 66, p. 48-55.

Drummond, A.D., Sutherland Brown, A., Young, R.J., and Tennant, S.J., 1976. Gibraltar - Regional metamorphism, mineralization, hydrothermal alteration and structural development; *in* Porphyry deposits of the Canadian Cordillera, (ed.) A. Sutherland Brown; Canadian Institute of Mining and Metallurgy, Special Volume 15, p. 195-205.

Grunsky, E., Lefebure, D., and Jones, L., 1996. Grade and tonnage data for selected deposit types; *in* Selected British Columbia Mineral Deposit Profiles, (eds.) D.V. Lefebure and T. Höy; British Columbia Geological Survey Open File 1996-13, p. 121–146.

Jones, S., 2015. 43-101 of the Gibraltar mine as of December 2014 http://sedar.com/FindCompanyDocuments.do and http://www.tasekomines.com/gibraltar/ID540174

Logan, J.M., Schiarizza, P., Struik, L.C., Barnett, C., Nelson, J.L., Kowalczyk, P., Ferri, F., Mihalynuk, M.G., Thomas, M.D., Gammon, P., Lett, R., Jackaman, W., and Ferbey, T. (compilers), 2010. Bedrock geology of the Quest map area, central British Columbia; Geoscience BC Report 2010-5, British Columbia Geological Survey, Geoscience Map 2010-1 and Geological Survey of Canada Open File 6476, scale 1:500 000.

Massey, N.W.D., MacIntyre, D.G., Desjardins, P.J., and Cooney, R.T., 2005. Digital Geology Map of British Columbia - Whole Province, British Columbia Ministry of Energy and Mines, GeoFile 2005-1.

Masumoto, Y., Enami, M., Tsuboi, M., and Hong, M., 2014. Magmatic zoisite and epidote in tonalite of the Ryoke belt, central Japan; European Journal of Mineralogy, v. 26, p.279-291.

Oliver, J., Crozier, J., Kamionko, M., and Fleming, J., 2009. The Gibraltar Mine, British Columbia. A billion tonne deep copper-molybdenum porphyry system: structural style, patterns of mineralization and rock alteration; Association for Mineral Exploration British Columbia, 2009 Mineral Exploration Roundup, Vancouver, British Columbia, Abstracts, p. 35-36.

Panteleyev, A., 1978. Granite Mountain project (93B/8); *in* Geological Fieldwork 1977, British Columbia Ministry of Energy and Mines, British Columbia Geological Survey, Paper 1978-1, p. 39-42.

Plouffe, A., and Ferbey, T., 2015. Till composition near Cu-porphyry deposits in British Columbia: Highlights for mineral exploration; *in* TGI 4 - Intrusion Related Mineralisation Project: New Vectors to Buried Porphyry-Style Mineralisation, (ed.) N. Rogers; Geological Survey of Canada, Open File 7843, p. 15-37.

Plouffe, A., Ferbey, T., and Anderson, R.G., 2014. Till composition and ice-flow history in the region of the Gibraltar Mine: developing indicators for the search of buried mineralization; Geological Survey of Canada, Open File 7592, poster.

Roache, T.J., Walshe, J.L., Huntington, J.F. Quigley, M.A., Yang, K., Bil, B.W., Blake, K.L., and Hyvarinen, T., 2011. Epidote-clinozoisite as a hyperspectral tool in exploration for Archean gold. Australian Journal of Earth Sciences, v. 58, p. 813-822.

Rukhlov, A.S., Plouffe, A., Ferbey, T., Mao, M., and Spence, J., 2016. Application of trace-element compositions of detrital apatite to explore for porphyry deposits in central British Columbia *in* Geological Fieldwork 2015, British Columbia Ministry of Energy and Mines, British Columbia Geological Survey, Paper 2016-1, p. 145-179.

Schiarizza, P., 2014. Geological setting of the Granite Mountain batholith, host to the Gibraltar porphyry Cu-Mo deposit, south-central British Columbia; *in* Geological Fieldwork 2013, British Columbia Ministry of Energy and Mines, British Columbia Geological Survey, Paper 2014-1, p. 95-110.

Schiarizza, P., 2015. Geological setting of the Granite Mountain batholith, south-central British Columbia; British Columbia Ministry of Energy and Mines, GeoFile 2015-5, poster.

Schmidt, M.W., and Poli, S., 2004. Magmatic epidote; *in* Epidote (eds.) Axel Libscher and Gerhard Franz; Reviews in Mineralogy and Geochemisty, v.56, p. 399-430.

Shannon, K.R., 1982. Cache Creek Group and contiguous rocks, near Cache Creek, British Columbia, Unpublished MSc thesis, University of British Columbia, 72 p.

Wilkinson, J.J., Chang, Z., Cooke, D.R., Baker, M.J., Wilkinson, C.C., Inglis, S., Chen, H., and Gemmell, B.J., 2015. The chlorite proximitor: A new tool for detecting porphyry ore deposits; Journal of Geochemical Exploration, v. 152, p. 10-26.